

## N95-11025

LIDAR MEASUREMENTS OF OZONE AND AEROSOL DISTRIBUTIONS DURING  
THE 1992 AIRBORNE ARCTIC STRATOSPHERIC EXPEDITION

Edward V. Browell<sup>1</sup>, Carolyn F. Butler<sup>2</sup>, Maria A. Fenn<sup>2</sup>, William B. Grant<sup>1</sup>, Syed Ismail<sup>1</sup>, and Arlen F. Carter<sup>1</sup>

<sup>1</sup>NASA Langley Research Center, Atmospheric Sciences Division, Hampton, Virginia 23681

<sup>2</sup>Science Applications International Corporation, Hampton, Virginia 23666

## ABSTRACT

The NASA Langley airborne differential absorption lidar system was operated from the NASA Ames DC-8 aircraft during the 1992 Airborne Arctic Stratospheric Expedition to investigate the distribution of stratospheric aerosols and ozone (O<sub>3</sub>) across the Arctic vortex from January to March 1992. Aerosols from the Mt. Pinatubo eruption were found outside and inside the Arctic vortex with distinctly different scattering characteristics and spatial distributions in the two regions. The aerosol and O<sub>3</sub> distributions clearly identified the edge of the vortex and provided additional information on vortex dynamics and transport processes. Few polar stratospheric clouds were observed during the AASE-II; however, those that were found had enhanced scattering and depolarization over the background Pinatubo aerosols. The distribution of aerosols inside the vortex exhibited relatively minor changes during the AASE-II. Ozone depletion inside the vortex was limited to  $\leq 20\%$  in the altitude region from 15-20 km.

## 1. INTRODUCTION

The first Airborne Arctic Stratospheric Expedition (AASE-I) was conducted during the winter of 1988-89, and results from this expedition established that the same chlorine-related chemistry that was responsible for O<sub>3</sub> depletion in the springtime Antarctic stratosphere was also occurring in the wintertime Arctic stratosphere [Turco et al., 1990; *Geophys. Res. Lett.*, 17, Number 4, 1990]. A second AASE campaign (AASE-II) was then conducted during the winter of 1991-92 to study the evolution of the dynamics, chemistry, and O<sub>3</sub> depletion associated with the wintertime Arctic vortex. In both of these expeditions, the NASA Langley Research Center's airborne differential absorption lidar (DIAL) system [Browell et al., 1983; Browell, 1989] was flown on the NASA Ames Research Center's DC-8 aircraft to make measurements of O<sub>3</sub> and aerosol profiles from about 1 km above the aircraft to altitudes of 23-26 km for O<sub>3</sub> and to above 27 km for aerosols [Browell et al., 1990a, 1990b].

The airborne DIAL system simultaneously transmits six laser beams at about 10 Hz in a zenith mode from the DC-8 for profile measurements of: O<sub>3</sub> concentrations using on- and off-line DIAL wavelengths of 301.5 and 311 nm, respectively; atmospheric backscatter ratios at 603 and 1064 nm; and aerosol depolarization ratios at 603 and 1064 nm. Large-scale distributions of these parameters were obtained in the Arctic stratosphere from January to March 1992 on long-range flights made each month from the NASA Ames Research Center (ARC), Moffett Field, California, to Anchorage, Alaska, to Stavanger, Norway, to Bangor, Maine, and then back to NASA ARC. Additional round-trip flights

north into the vortex were made each month from either Stavanger or Bangor depending on the location of the vortex that month. Each flight lasted for about 10 hours and covered about 8000 km. Eleven of these flights permitted measurements across the edge of the Arctic vortex.

This paper discusses the procedures used in making the lidar measurements of O<sub>3</sub> and aerosols and the results of observations of Pinatubo aerosols, PSCs, and O<sub>3</sub> made with the airborne DIAL system in the wintertime Arctic stratosphere during the AASE-II. These results are related to the measurements made during the AASE-I campaign [Browell et al., 1990a, 1990b].

## 2. LIDAR MEASUREMENT PROCEDURES

Ozone

The O<sub>3</sub> DIAL technique [Browell et al., 1983, 1985] has been used in many airborne lidar atmospheric investigations over the past 12 years. This technique and the results of a number of field experiments have been previously discussed in detail for the measurement of O<sub>3</sub> in the troposphere [Browell et al., 1983, Browell, 1989] and in the stratosphere [Browell, 1989; Browell et al., 1988, 1990a, 1990b]. The on- and off-line laser wavelengths used for the DIAL measurements during the AASE campaigns were 301.5 and 311 nm, respectively. During the AASE-I campaign, the large-scale ( $\geq 1$  km) O<sub>3</sub> measurements of the airborne DIAL system were found to be within 10% of the O<sub>3</sub> measurements made from aircraft, balloons, and satellites [Margitan et al., 1989].

The O<sub>3</sub> mixing ratio profile is determined from the DIAL-derived O<sub>3</sub> concentration profile by dividing the O<sub>3</sub> number density at each altitude by the atmospheric number density derived from the closest 12-hour National Meteorological Center (NMC) meteorological analysis for the same location. Since the O<sub>3</sub> mixing ratio is conserved in adiabatic processes, the O<sub>3</sub> mixing ratio is the preferred quantity for examining the possible decrease in O<sub>3</sub> due to chemical processes.

Aerosols

The lidar backscatter return from the atmosphere can be calibrated to determine the atmospheric scattering ratio (R<sub>T</sub>) at a specific altitude, where R<sub>T</sub> is defined as the sum of the aerosol and molecular scattering divided by the molecular scattering. To determine the atmospheric scattering ratio profile, the relative molecular scattering profile needs to be determined for each observation. To do this, a clean (aerosol-free) region for each flight is identified along the flight track at an altitude above ~18 km that has sufficient signal-to-noise for an accurate estimate of the molecular scattering. The relative molecular scattering profile is then calculated by normalizing the molecular

number density profile to the relative scattering in the clean region. The relative molecular scattering profile at any other location is then calculated using: the molecular number density profile at the new location; the molecular scattering normalization obtained in the clean region; and the relative change in the laser energy or other lidar system parameters from the normalization location. The same procedure is adopted at both 603 nm (VIS) and 1064 nm (IR), and in this analysis, it is assumed that extinction of the lidar signal due to atmospheric scattering and absorption is negligible.

The atmospheric depolarization at 603 and 1064 nm was measured from two orthogonally polarized lidar returns probing the same atmospheric volume within 300  $\mu$ s. One detector system for each wavelength is used to detect the parallel backscattered return from the first pulse and then the perpendicular backscattered return from the second pulse. The total atmospheric depolarization ( $D_T$ ) is defined as the perpendicular backscattered return ( $S_S$ ) divided by the parallel return ( $S_p$ ), or  $D_T = S_S/S_p$ . When the atmosphere has a low amount of aerosol scattering compared to molecular scattering, the total atmospheric depolarization defined above reflects more the depolarization from the molecules than from the aerosols. To determine the depolarization from the aerosol component in the lidar returns, the molecular component is subtracted from the perpendicular and parallel returns. The molecular components of both the perpendicular ( $M_S$ ) and parallel ( $M_p$ ) returns can be determined using the same normalization technique described above for the determination of the atmospheric scattering ratio distribution. The aerosol depolarization ( $D_A$ ) can then be written as  $D_A = (S_S - M_S)/(S_p - M_p)$ . A detailed discussion of this procedure is given by Browell et al. [1990a].

### 3. AEROSOL AND OZONE MEASUREMENTS

#### Pinatubo Aerosols

Aerosols from the Mount Pinatubo eruption in July 1991 were observed across the entire Arctic region throughout the AASE-II campaign. Outside the Arctic vortex the Pinatubo aerosols were found to extend over the 12-26 km altitude range with an aerosol peak near 21 km. Figure 1 presents an example of the atmospheric scattering ratio profile found outside the Arctic vortex. While the peak scattering ratio in Figure 1 is about 10, the average maximum value of the IR and VIS atmospheric scattering ratios were about 12 and 6, respectively. These values are about half of the values observed for the Pinatubo aerosols at low latitudes (5-20°N) during the NASA Pacific Exploratory Mission (PEM-West) conducted in September-October 1991. The average ratio of the IR to VIS aerosol scattering ratios was found to be about 2.2 for the peak Pinatubo layer in both the low latitudes and outside the Arctic vortex. This ratio represents an aerosol backscatter wavelength dependence ( $\alpha$  in  $\lambda^{-\alpha}$ ) of about 2.6. This generally indicates an abundance of small size aerosols ( $\sim 1 \mu$ m in diameter).

The Pinatubo aerosol distribution near the center of the Arctic vortex extended from the tropopause to about 17 km in January and to about 18-18.5 km in February and March. An example of the atmospheric distribution found inside the Arctic vortex in January is shown in Figure 2. The center of the Pinatubo layer in the vortex remained at about 15 km for the entire period. The average IR and VIS atmospheric scattering ratios at the peak of the layer were estimated to be about 5 and 3, respectively. The average ratio of the IR to VIS aerosol scattering ratios inside the vortex was also found to be about 2 with about the same resulting backscatter wavelength dependence that was found outside the vortex. The distribution and scattering properties of the Pinatubo aerosols were significantly different across the vortex edge during

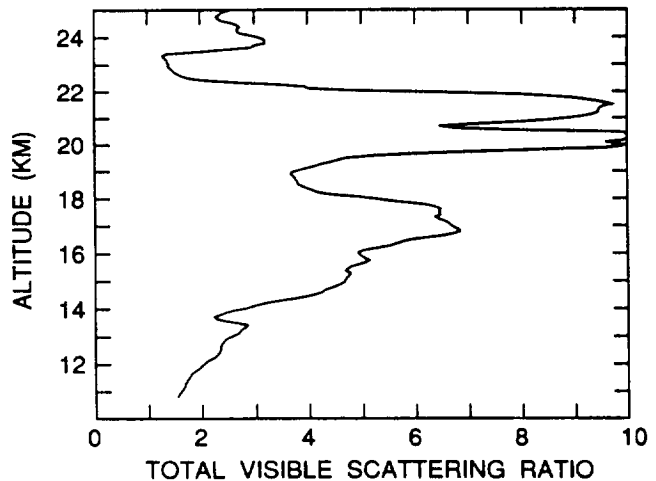


Fig. 1. Aerosol distribution observed outside the Arctic vortex at 73.7°N/148°W on January 16, 1992.

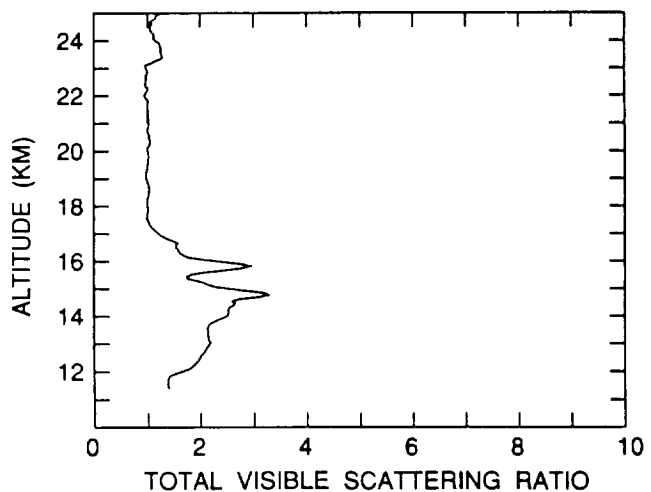


Fig. 2. Aerosol distribution observed inside the Arctic vortex at 81.1°N/138°W on January 16, 1992.

January; however, in February and March, aerosol layers outside the vortex in the 18-24-km range began to be slowly transported toward the center of the vortex. In general, the start of the aerosol transition region coincided with the location of the vortex edge predicted by the potential vorticity (PV) distribution on the 440 K potential temperature surface.

Low depolarization (<2%) was measured across the main portion of the Pinatubo layer both outside and inside the vortex, and this did not change over the campaign. This low depolarization is consistent with the small size and nearly spherical nature of the sulfuric acid aerosols that dominate the composition of the Pinatubo layer. Frequent enhancements in the aerosol depolarization of 4-6% were found at the bottom of the Pinatubo layer (generally below 15 km) where the aerosol scattering ratios were low (<2). These are thought to be caused by

a low density of larger nonspherical aerosols possibly resulting from the subsidence of large crustal particles.

#### Polar Stratospheric Clouds

Polar stratospheric clouds were observed on only one mission during the AASE-II. On January 19, 1992, PSCs were observed near the top of the Pinatubo layer (near 22 km) in a cold region (<195 K) just outside the vortex between Norway and Iceland. A tropospheric high-pressure system created a dome of cold temperatures which forced the air in the lower stratosphere to rise by several kilometers. Cirrus clouds were observed as high as 14 km in the center of this region. Isolated PSCs in the 19-22-km region exhibited enhanced depolarization (>25%) and large peak IR and VIS atmospheric scattering ratios of about 50 and 9.5, respectively. These characteristics are similar to the Type II water ice PSCs observed during the AASE-I campaign in January-February 1989. The backscatter wavelength dependence of these aerosols was about 0.9, and this indicates that the aerosols were generally greater than 2  $\mu\text{m}$  in diameter. There was also a low-level increase in aerosol scattering across the entire Pinatubo aerosol layer between 14-22 km in this cold region. This may have resulted from the deposition of nitric acid onto the Pinatubo aerosols.

#### Ozone

The O<sub>3</sub> distribution observed over the altitude range from 12-25 km with the lidar system showed a clear transition across the Arctic vortex edge with the O<sub>3</sub> profile generally decreasing in altitude by about 1.5 km upon going from outside to inside the vortex. The location of the vortex edge determined from the O<sub>3</sub> distribution corresponded closely with the location of the edge derived from the potential vorticity analysis on the 440 K potential temperature surface. There was a good correlation in the general vortex edge location as determined by the lidar O<sub>3</sub> and aerosol distributions; however, the lower-resolution O<sub>3</sub> distribution did not show the small-scale structure observed in the high-resolution aerosol data.

There was only a minor influence of the presence of the Pinatubo aerosols on the DIAL-derived O<sub>3</sub> profiles. The vertical O<sub>3</sub> distribution outside the vortex showed an increase in the O<sub>3</sub> mixing ratio from about 0.4 ppmv (parts per million by volume) at 14 km to about 4.8 ppmv at 23 km with a slight depression in the O<sub>3</sub> distribution across the Pinatubo aerosol layer. This low level of decrease is difficult to quantify because there was no clean region observed for comparison. Inside the vortex in the region of the highest potential vorticity, the O<sub>3</sub> distribution was found to have a constant increase from about 1 ppmv at 14 km to about 3.6 ppmv at 21 km. Figure 3 presents the O<sub>3</sub> mixing ratio profiles found inside the Arctic vortex on two flights during January 1992. No apparent trend in the DIAL derived O<sub>3</sub> profiles were found to be associated with the low level of Pinatubo aerosols inside the vortex.

Between January and February, the only change that was detected in the O<sub>3</sub> profile was a decrease of less than 20% in the region from 16 to 19.5 km (see Figure 4). Since this decrease was not associated with an increase in aerosol scattering which would have indicated extra-vortex air, it is thought to be associated with chemical O<sub>3</sub> depletion in the vortex. The March O<sub>3</sub> profiles showed a decrease of  $\leq 10\%$  over the same altitude range when compared to the January O<sub>3</sub> profiles. No other obvious O<sub>3</sub> changes were observed inside the vortex over the period of the AASE-II.

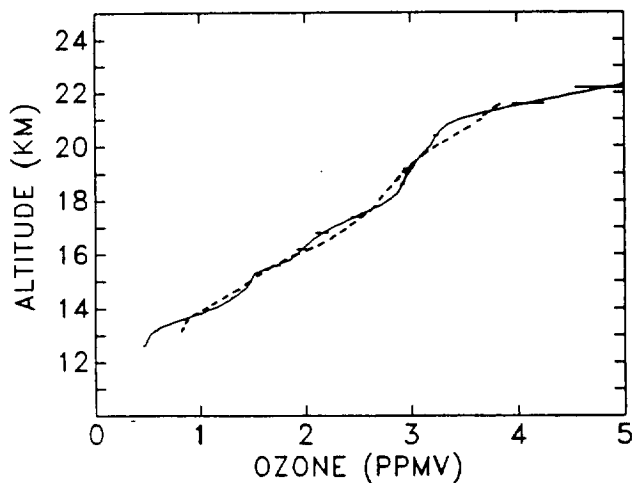


Fig. 3. Comparison of average O<sub>3</sub> mixing ratio profiles observed inside the Arctic vortex on January 16, 1992, (solid line) near 81°N/140°W and on January 22, 1992, (dashed line) near 60°N/69°W.

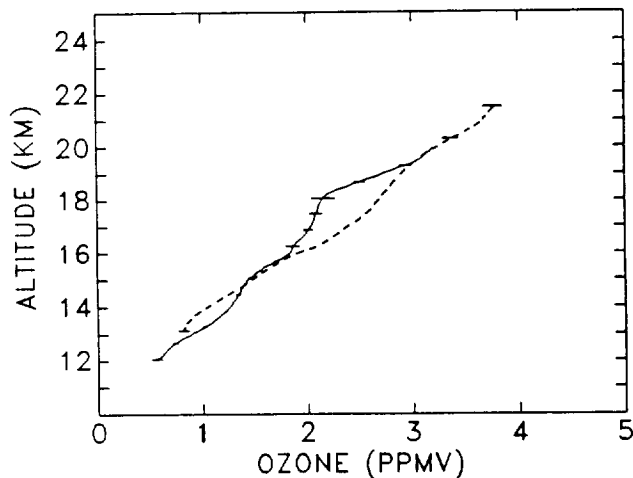


Fig. 4. Comparison of average O<sub>3</sub> mixing ratio profiles obtained inside the Arctic vortex on February 22, 1992, (solid line) near 63°N/62°W and on January 22, 1992, (dashed line) near 60°N/69°W.

#### 4. CONCLUSIONS

The dynamics of the Arctic vortex was reflected in the differences observed in the distribution and scattering characteristics of the Pinatubo aerosols across the edge of the Arctic vortex. The amount of Pinatubo aerosols that reached the Arctic prior to the establishment of the vortex in the fall of 1991 was clearly less than the amount that was observed outside the vortex in January 1992. The O<sub>3</sub> distribution across the edge of the vortex also showed a relative descent of about 1.5 km from outside to inside the vortex. This is a result of descending motion in the vortex during the winter. The region of the maximum O<sub>3</sub> gradient compared well with the edge of the vortex as defined by the potential vorticity analysis and the abrupt change in the Pinatubo aerosol distribution. Air masses were sometimes observed in the lower stratosphere (typically <20 km) that were thought to be "inside the vortex"; however, they had aerosol scattering characteristics similar to extra vortex air. These air masses also had O<sub>3</sub> levels that were found in air with similar aerosol loading outside the vortex. A closer examination of these cases showed that these air masses were also associated with low potential vorticity regions. The vortex had been distorted in these regions, and based on our March 1992 aerosol and O<sub>3</sub> measurements in the vortex, it was found that these air masses had not been irreversibly transported into the vortex.

Inside the Arctic vortex there was no evidence of descent indicated in the lidar aerosol or O<sub>3</sub> data below 23 km from January to March 1992. The aerosol layer inside the high potential vorticity region of the vortex showed an increase in the top of the layer from 17 to 18.5 km over the period of the lidar flights. This reflects mixing inside the vortex at these lower altitudes. Over the time of the airborne lidar measurements, the center of the aerosol layer in the vortex stayed at about 15 km. The only change in O<sub>3</sub> observed inside the vortex during AASE-II was in the 16-19.5 km region. A maximum O<sub>3</sub> decrease of <20% from the January profile was found at 18 km in late February. Since this is not associated with a region of enhanced aerosol scattering, it is thought that this decrease in O<sub>3</sub> is associated with chemical O<sub>3</sub> depletion in the vortex. The measurements in March also showed evidence of reduced O<sub>3</sub> (<10%) in this same altitude region. The amount of O<sub>3</sub> depletion was less than expected due to the warmer than usual temperatures this winter in the Arctic stratosphere, as evidenced by the few PSCs that were observed this year compared to previous years.

#### 5. ACKNOWLEDGMENTS

The authors thank N. S. Higdon, M. L. Jones, M. N. Mayo, W. J. McCabe, B. L. Meadows, and J. A. Williams of the Lidar Applications Group in the Atmospheric Sciences Division at the NASA Langley Research Center for their assistance in developing the comprehensive measurement capabilities of the airborne DIAL system, integrating the system into the DC-8, and operating the lidar system in the field. We also appreciate the assistance of S. A. Kooi, S. D. Mayor, and G. D. Nowicki in reducing the lidar data and producing the color data plots. This research was supported by NASA's Upper Atmospheric Research Program.

#### REFERENCES

- Browell, E. V., Differential absorption lidar sensing of ozone, *Proc. IEEE*, **77**, 419-432, 1989.
- Browell, E. V., A. F. Carter, S. T. Shipley, R. J. Allen, C. F. Butler, M. N. Mayo, J. H. Siviter, Jr., and W. M. Hall, NASA multipurpose airborne DIAL system and measurements of ozone and aerosol profiles, *Appl. Opt.*, **22**, 522-534, 1983.
- Browell, E. V., S. Ismail, and S. T. Shipley, Ultraviolet DIAL measurements of O<sub>3</sub> profiles in regions of spatially inhomogeneous aerosols, *Appl. Opt.*, **24**, 2827-2836, 1985.
- Browell, E. V., L. R. Poole, M. P. McCormick, S. Ismail, C. F. Butler, S. A. Kooi, M. M. Szedlmayer, R. Jones, A. Krueger, and A. Tuck, Large-scale variations in ozone and polar stratospheric clouds measured with airborne lidar during formation of the 1987 ozone hole over Antarctica, paper presented at the NASA Polar Ozone Workshop, Snowmass, Colorado, May 9-13, 1988, abstract in *Polar Ozone Workshop*, pp. 61-63, *NASA Conf. Publ.*, CP-10014, 1988.
- Browell, E. V., C. F. Butler, S. Ismail, P. A. Robinette, A. F. Carter, N. S. Higdon, O. B. Toon, M. R. Schoeberl, and A. F. Tuck, Airborne lidar observations in the wintertime Arctic stratosphere: Polar stratosphere clouds, *Geophys. Res. Lett.*, **17**, 385-388, 1990a.
- Browell, E. V., C. F. Butler, S. Ismail, M. A. Fenn, S. A. Kooi, A. F. Carter, A. F. Tuck, O. B. Toon, M. H. Proffitt, M. Loewenstein, M. R. Schoeberl, I. Isaksen, and G. Braathen, Airborne lidar observations in the wintertime Arctic stratosphere: Ozone, *Geophys. Res. Lett.*, **17**, 325-328, 1990b.
- Margitan, J., et al., Intercomparison of ozone measurements over Antarctica, *J. Geophys. Res.*, **94**, 16,557-16,569, 1989.
- Turco, R., A. Plumb, and E. Condon, The Airborne Arctic Stratospheric Expedition: Prologue, *Geophys. Res. Lett.*, **17**, 313-316, 1990.